

## TURBULENCE GENERATED BY WAVE BREAKING ON BEACH

by

T. Sakai<sup>1</sup>, Y. Inada<sup>2</sup> and I. Sandanbata<sup>3</sup>

### ABSTRACT

Horizontal and vertical velocities are measured with a hot-film anemometer(HFA) and a two-component laser-doppler velocimeter(LDV) in surf zones on uniform slopes of about 1/30 in two wave tanks. The turbulence generated by wave breaking is detected from the records. Following three aspects of the turbulence are discussed : (1) the distribution of the turbulence intensity in the surf zone, (2) the variation of the vertical distribution of the turbulence during one wave period and (3) the variation of the Reynolds stress during one wave period. It is found that the pattern of the distribution of the turbulence in the surf zone depends on the breaker type. A model is proposed, by extending the turbulent wake theory, to explain the variation of the vertical distribution of the turbulence during one wave period.

### 1. INTRODUCTION

It is recognized that the turbulence generated by wave breaking in surf zone plays an important role in various phenomena such as generation of longshore current, suspension of sediment and dispersion of material in surf zone.

Peregrine and Svendsen(1978) proposed a qualitative model for the flow field in spilling breaker. They concluded that the turbulent flow, immediately following the breaking, resembles a turbulent mixing layer.

Battjes and Sakai(1981) measured a velocity field in a steady breaker generated behind a wing inserted in a uniform open channel flow. The mean flow, the turbulent intensity, the Reynolds stress and their decays with distance downward and downstream were discussed in comparison with the turbulent shear layer and turbulent wake theories. They concluded that the whole velocity field resembles the turbulent wake rather than the turbulent shear layer.

The steady breaker, in which Battjes and Sakai measured the velocities,

---

1) Assoc. Prof., Dept. of Civil Engg., Kyoto Univ., Kyoto, Japan

2) Engineer, Tobishima Cooperation, Tokyo, Japan

3) Graduate student, School of Civil Engg., Kyoto Univ., Kyoto, Japan

is not progressive but standing. Stive(1980) measured the velocity due to progressive breaking waves in a surf zone on a uniform slope of  $1/40$  in a wave tank by using a laser-doppler velocimeter. He also found a wake type flow in the region behind the crest. Flick, Guza and Inman(1981) measured the velocity in a surf zone on a uniform slope of  $1/35$  in a wave tank by using a hot-film anemometer. They discussed a difference of the turbulence due to the breaker type.

The conclusions and discussions in above mentioned two works are limited to few experimental conditions. In this study, the velocity fields are measured, under conditions different from those of their works, in surf zones on uniform slopes in two wave tanks by using a hot-film anemometer and a two-components laser-doppler velocimeter. At first, the effects of the breaker type on the overall turbulence distribution in the surf zone are discussed.

Secondly the variation of the vertical distribution of the turbulence during one wave period is discussed. A model is proposed, by extending the turbulent wake theory, in order to explain the variation. Finally a cross product of the simultaneous horizontal and vertical velocity fluctuations is calculated. The variation of this cross product during one wave period and its physical meaning are discussed.

## 2. EXPERIMENTS

### 2.1. Arrangements

The experiments were done in two wave tanks. Two wave tanks have nearly the same dimensions. The length is about 30m, the width is about 50cm and the height is about 70cm. A uniform slope of about  $1/30$  was installed in the tanks. The still water depth in the uniform depth part in front of the slope was always 35cm(see Fig.1). X-axis is taken shoreward from the breaking point. Z-axis is taken upward above the still water level. The experimental conditions are listed in Table 1.

The letters "H" and "L" in the case number indicate that the hot-film anemometer and laser-doppler velocimeter was used in the case respectively.  $h_1$  is the still water depth in the uniform depth part in the tank,  $i$  is the slope and  $T$  is the wave period.  $H_0/L_0$  is the deep-water wave steepness calculated from the wave height in the uniform depth part or at the breaking point.  $h_b$  is the still water depth at the breaking point,  $H_b$  is the wave height at the breaking point, and  $W$  is the width of the surf zone between the breaking point and the still water line (see Fig.1). The word "transient" in the column of breaker type means that the breaker type was a transient type between the spilling and plunging breakers. "HFA" and "LDV" mean hot-film anemometer and laser-doppler velocimeter respectively.

### 2.2. Measurements

The water surface elevation was measured at the breaking point and

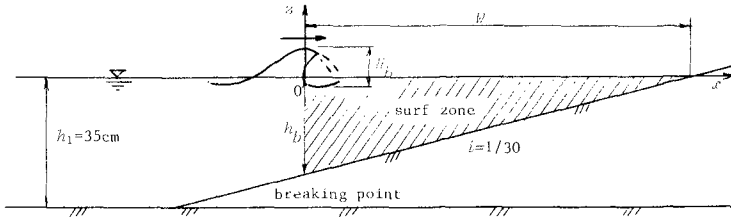


Fig.1 Experimental Arrangements

Table 1 Experimental Conditions

case	$h_1$ (cm)	$i$	$T$ (sec)	$H_0/L_0$	$h_B$ (cm)	$H_B$ (cm)	$w$ (cm)	breaker type	instrument
H1	35.0	1/31	1.00	0.088	19.4	13.3	600	spilling	HFA
H2	35.0	1/28	1.16	0.066	17.7	12.8	490	spilling	HFA
L	35.0	1/31	1.17	0.063	18.0	12.8	530	spilling	LDV
H3	35.0	1/31	1.32	0.032	14.5	10.4	450	transient	HFA

the velocity measuring point with two capacitance-type wave gauges. In the cases H1 and H3, the water surface elevation was measured in the uniform depth part too.

The hot-film anemometer is DISA type 55M01, and the probe is DISA type 55R13. The hot-film probe was calibrated by using a vertically oscillating plate in still water to which the probe was attached. This probe has a vertical sensor of cylinder type and measures the velocity of the on-offshore direction. In the cases H1 and H3, in which the hot-film anemometer was used, the on-offshore velocity was measured at about 30 points under the level of the wave trough in the surf zone. The recording time at one point was 90sec. In the case H2, it was measured at about 40 points under the still water level in the surf zone. The recording time at one point was 60sec.

The two-components laser-doppler velocimeter is KANOMAX optical system 8143S, and the signal processor is KANOMAX model 8015 of tracker type. It can measure two components of oscillatory flow velocity simultaneously. The mode of operation was the forward scatter fringe mode. The on-offshore and vertical velocities were measured at about 40 points in the case L under the still water level in the surf zone. The recording time at one point was 60sec.

All outputs from the wave gauges and the velocity meter were recorded in a analog magnetic recorder simultaneously. In the case L, the dropout signals from the laser-doppler velocimeter were also recorded.

### 3. DATA ANALYSIS

#### 3.1. Distribution of Turbulence in Surf Zone(Cases H1 and H3)

In the cases H1 and H3, the data in the analog recorder were A-D converted every 0.01sec during 60sec for each measuring point. The first part of 24sec in the digital data was plotted graphically. Fig.2 shows two examples of the time profiles of the water level and the on-offshore velocity. In general, hot-film anemometer can not feel the change of the velocity direction. So the output of the measured velocity is rectified.

The figure (1) shows the time profiles at the breaking point. It is clear that the significant turbulence does not yet exist at the breaking point especially in the crest phase. On the other hand, within the surf zone, it is not so easy to find the instance when the direction of the water particle velocity changes in the time record due to the high turbulence(the figure (2)). Waves, in which the instance of the direction change was possible to find, were selected in the record. At most 90% of the waves during 24sec were selected.

The time profile of the velocity varies wave to wave. Turbulence defined as the deviation from the ensemble average of many waves(Stive, 1980) includes above mentioned velocity profile variation. Considering this fact, the measured velocity was smoothed with a moving average method for each selected wave. The time interval of average was 0.1sec.

A root-mean-square of the deviation  $u'$  from the smoothed velocity  $u_w$  was calculated for each selected wave. This was done separately for the phase of onshore velocity and the phase of offshore velocity(see Fig.3). They are called the horizontal turbulent intensities at the onshore velocity phase and the offshore velocity phase, and are expressed with symbols " $u'_{rms,c}$ " and " $u'_{rms,t}$ " respectively.

#### 3.2. Variation of Vertical Distribution of Turbulence during One Wave Period(Case H2)

As well as in the cases H1 and H3, the data in the analog recorder were A-D converted every 0.01sec for each measuring point. The first part of 24sec in the digital data was plotted graphically. In order to discuss the variation of the turbulence during one wave period, the velocity record during the full length of 24sec, which contains about 20 waves, was smoothed with the same moving average method as in the cases H1 and H3(see Fig.4).

One wave period was divided into 12 sections of 0.1sec. The first section starts at the phase when the water surface crosses the still water level upward. The length of the last section is shorter than 0.1sec, because the wave period of the case H2 is 1.16sec. Each section of each wave contains 10 data of the deviation  $u'$  from the smoothed velocity  $u_w$ , except for the last section. For each section, a root-mean-square of the deviation  $u'$  of all waves was calculated. This is expressed with a symbol " $u'_{rms}(t)$ ".

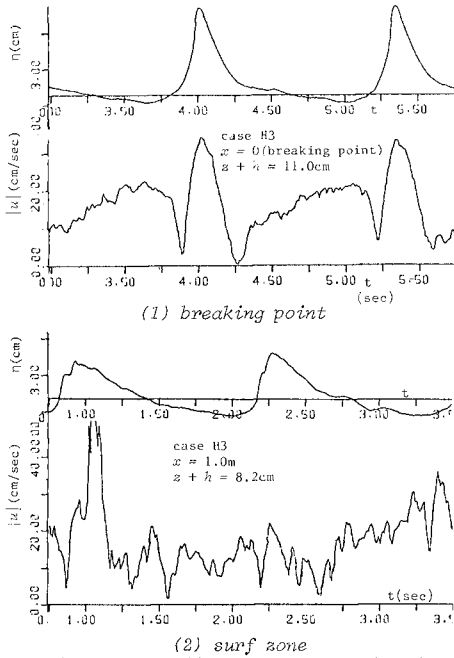


Fig. 2, (1), (2) Time Profiles of Water Level and On-offshore Velocity Measured with Hot-Film Anemometer

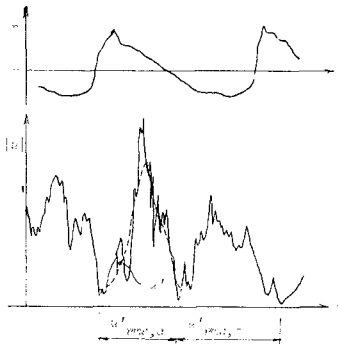


Fig. 3 Horizontal Turbulent Intensities at Onshore and Offshore Velocity Phases  $u'_{rms,c}$  and  $u'_{rms,t}$

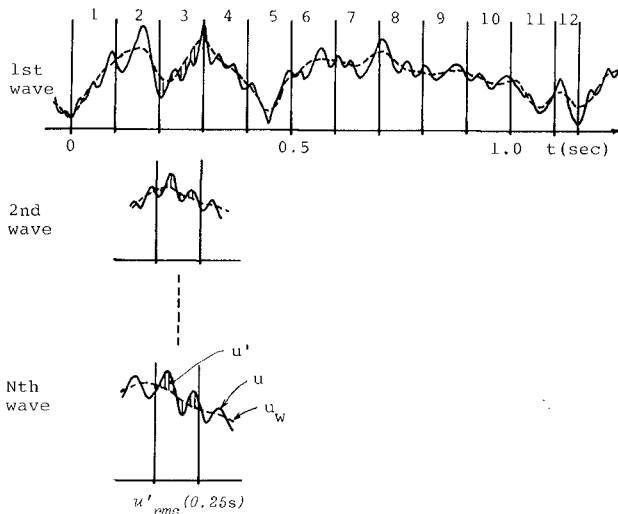


Fig.4 Variation of Turbulent Intensity " $u'_{rms}(t)$ "

### 3.3. Cross Product of On-offshore and Vertical Deviations $u'$ and $w'$ (Case L)

In the case L, the data in the analog recorder were A-D converted every 0.01sec during 48sec for each measuring point. The water level variations at the breaking point and the velocity measuring point, the on-offshore and vertical velocities and their dropout signals of 48sec were plotted graphically.

In general, laser-doppler velocimeter can not get any information about the flow velocity when no particle is detected by the LDV system. The situation of such no velocity information is called "signal dropout". The signal processor was operated in the so-called track-and-hold mode. The output from the signal processor keeps the value just before the signal dropout(see Fig.5).

The signal dropout occurs due to several causes. At the measuring point above the trough level, in the trough phase, the laser beam goes out from the water between two glass walls of the tank. Then the dropout occurs. It occurs also when the air bubbles interrupt the beams. The time intervals when no signal dropout occurs were selected from the plotted time profiles for the on-offshore and vertical velocities.

The on-offshore and vertical velocities in the no-dropout intervals were smoothed with the same moving average method as in the cases H1, H2 and H3. The product of the simultaneous on-offshore and vertical deviations  $u'$  and  $w'$  from the smoothed velocities were calculated only

in the time intervals when no dropout occurs both in the on-offshore and vertical velocities(see Fig.5).

The value of the cross product of  $u'$  and  $w'$  at every 0.01sec in each no dropout interval was smoothed again with the moving average method of 0.1sec. This smoothed value is expressed with a symbol " $\overline{u'w'(t)}$ ".  $-\overline{u'w'(t)}$  is called Reynolds stress here. As the signal dropout occurs sometimes, there are waves in which the data of  $-\overline{u'w'(t)}$  are lacked in some part of one wave period.

The Reynolds stress  $-\overline{u'w'(t)}$  was ensemble averaged at every 0.01sec for all waves during 48sec. This ensemble averaged Reynolds stress is expressed with a symbol " $\langle -\overline{u'w'(t)} \rangle$ ". As mentioned above, there are waves in which the data are lacked in some part of one wave period. Therefore, the number of the ensemble averaging is, in general, equal to or less than the number of total waves during 48sec(about 40).

The time interval of one wave was defined as from the phase 0.5sec after the crest of the preceeding wave to the phase 0.5sec after the crest of the wave. The wave period of the individual wave varies wave to wave. So, near the end of one wave period, the number of the ensemble averaged data decreases rapidly.

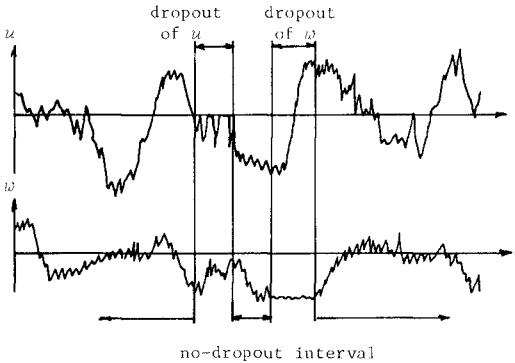


Fig.5 Signal Dropout of Laser-Doppler Velocimeter

#### 4. DISTRIBUTION OF TURBULENCE IN SURF ZONE

##### 4.1. Results

Fig.6,(1) shows the distribution of the horizontal turbulent intensities at the onshore velocity phase and the offshore velocity phase  $u'_{rms,c}$  and  $u'_{rms,t}$  in the surf zone in the case H1. In the figure, the range of scatter of the value is indicated by connecting the maximum and minimum values of each measuring point. The upper figure shows the on-offshore variation of the measured value at the highest measuring point. Fig.6,(2) shows the similar result in the case H3.

##### 4.2. Error Estimate

In these two cases, the hot-film anemometer was used. The measured values contain some errors. The first error comes from the uncertainty of the calibration curve of the hot-film anemometer. The calibration curve itself has the error of 3cm/sec. This error influences the smoothed velocity  $u_w$  directly. But it is thought that it does not influence the deviation  $u'$  defined as  $u - u_w$  so much.

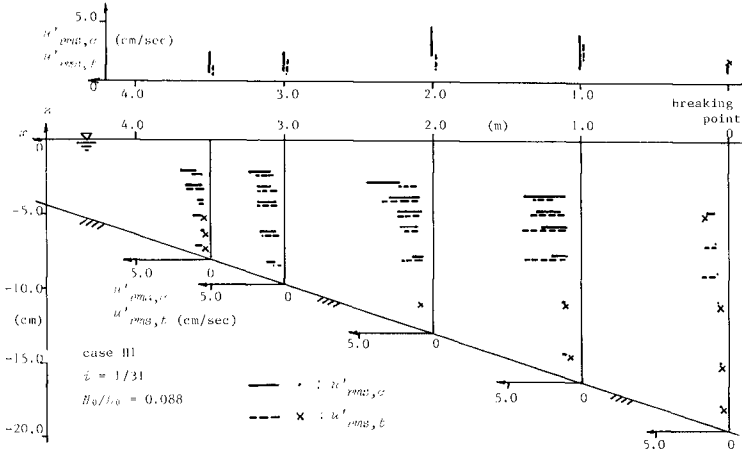
Another possible cause is the vibration of the probe mounting arm. The natural frequency of the arm was increased to more than 50Hz by shortening the length of the arm. So the fluctuation in the velocity due to the vibration was separated from the turbulence, the frequency of which is thought to be lower than 50Hz.

The probe may feel the vertical component of the velocity too especially near the phase when the on-offshore component becomes 0. This was already discussed(Isobe et al., 1979). It is found, using their result, that the error is about 1cm/sec. The ambiguity in the decision of the phase when the water particle velocity changes its direction is thought not to influence the mean value  $u'_{rms}$  so much.

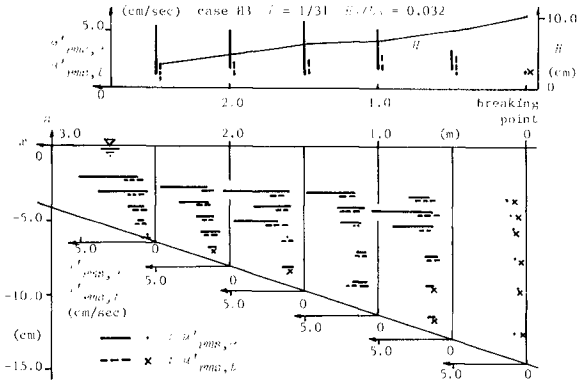
The value of the turbulence defined as the deviation from the smoothed velocity calculated by using the moving average method has one inherent error. The smoothed curve can not follow the abrupt change of the water particle velocity itself at the crest(see Fig.1,(1)). In fact, Fig.6 shows the turbulence of about 1cm/sec at the breaking point. This means that the value of  $u'_{rms,c}$  contains the error of 1cm/sec.

The severest error comes from the air bubble interruption of the probe. At present, nothing is done to separate the effect of the air bubble interruption from the velocity measured by using the hot-film anemometer. Only one thing being done to reduce this error was to limit the measuring points under the trough level where the concentration of the air bubble is not so high. Therefore it is impossible to estimate this error quantitatively. The measured value is thought to contain this error to some extent.

##### 4.3. Discussions



(1) case H1



(2) case H3

Fig. 6, (1), (2) Distribution of Horizontal Turbulent Intensities at Onshore and Offshore Velocity Phases  $u'_{rms,c}$  and  $u'_{rms,t}$

From Fig.6, it is found that the turbulent intensity varies largely wave to wave especially in the case H3, in which the breaker type was a transient type from spilling to plunging. The intensity is larger in the case H3 than in the case H1 in which the breaker type was spilling. It should be noticed that the breaking wave height  $H_b$  is smaller than that of the case H1 (see Table 1).

As already seen in Fig.2,(1), the significant turbulence does not exist at the breaking point. The turbulence begins to grow after the waves propagate some distance from the breaking point. In the case H1, the turbulence damps after it reaches a maximum. But in the case H3, it does not damp so much at least in the measurement region. The wave height  $H$  itself decreases monotonically even in the case H3.

The turbulent intensity is larger in the upper part than near the bottom especially in the case H3. It means that the turbulence generated by wave breaking does not penetrate into the lower part of the water body near the bottom. In the case H3, the turbulent intensity at the offshore velocity phase  $u'_{rms,t}$  is smaller than that at the onshore velocity phase  $u'_{rms,c}$ .

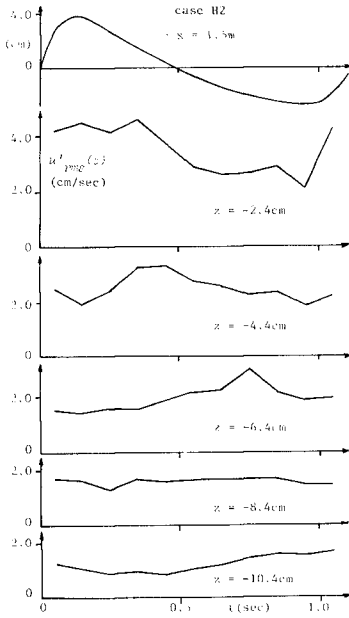
#### 5. VARIATION OF VERTICAL DISTRIBUTION OF TURBULENCE DURING ONE WAVE PERIOD

Fig.7,(1) shows one example of the variation of the horizontal turbulent intensity  $u'_{rms}(t)$  during one wave period in the case H2. The  $\langle \eta \rangle$  curve shows an ensemble mean of the time profile of about 20 waves. In this figure  $t$ -axis does not coincide with the still water level. Fig. ,(2) shows one example of another representation of the variation of the turbulent intensity during one wave period. In this figure, contour lines are used.

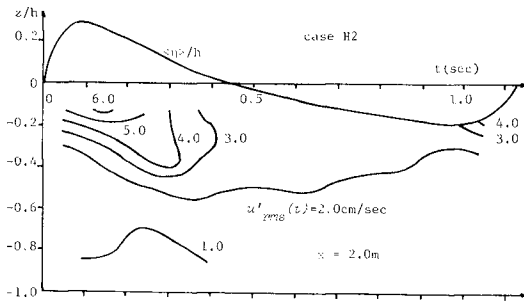
In the case H2, the hot-film anemometer was used. So the measured value contains the same errors as those in the cases H1 and H3. The velocity measurement was done also at the still water level. But, to reduce the error due to the air bubble interruption, the data at the still water level were not used in Fig. .

In this case, the velocity record during the full length of 24sec was smoothed. Therefore, the error due to the fact that the smoothed curve can not follow the abrupt change may occur also near the phase when the water particle velocity changes its direction. At such phase, the velocity becomes zero, and the rectified output drops abruptly to zero. But, as seen in Fig. ,(1), no effect of this error can be seen at the zero crossing phases.

As seen in Fig. ,(1), the phase of the peak in the curve of the variation of the turbulent intensity delays in the downward direction. This is also shown in the contour lines in the figure (2). The similar trend can be seen in Fig.8 of Stive(1980) too.



(1) 1.5m shoreward from breaking point



(2) 2.0m shoreward from breaking point

Fig. 7, (1), (2) Variation of Horizontal Turbulent Intensity  $u'_{rms}(t)$  during One Wave Period

## 6. MODELING OF TURBULENCE VARIATION DURING ONE WAVE PERIOD

Fig.8 shows the turbulence variation during one wave period in form of time series of the vertical profile of turbulent intensity, at two positions 1.5m and 2.0m shoreward from the breaking point in the case H2. The crosses indicate the measured values.

The vertical profile of the turbulent intensity resemble that measured by Battjes and Sakai(1981) under an air entraining turbulent water surface generated behind a wing inserted in an open channel flow(see Fig.3 of their paper). The trend of the variation during one wave period in Fig.8 also resembles the streamwise variation of the vertical profile measured by Battjes and Sakai.

They showed that the streamwise variations of the mean velocity defect near the water surface, the length scale of the vertical profile and the turbulent intensity are explained by the turbulent wake theory(Tennekes and Lumley, 1972). In the following, it is tried to explain the turbulence variation during one wave period shown in Fig.8 by extending the turbulent wake theory.

### 6.1. Turbulent Wake Theory(Tennekes and Lumley, 1972)

Turbulent wake belongs to free turbulence as well as turbulent jet and turbulent shear layer(see Fig.9). Following assumptions are made in the turbulent wake theory : 1) The length scale in the streamwise direction is larger than the length scale  $l$  in the lateral direction, 2) Reynolds number is large, and 3) The order of the velocity defect  $U$  is same as the order of the turbulence. The equations of motion are simplified according to these assumptions.

One characteristic feature of free turbulence is that there is no characteristic length such as the water depth or the channel width. Then the velocity profile in the lateral direction are similar in the streamwise direction("self preservation"). Therefore the velocity  $U$  and the Reynolds stress are functions of only the lateral distance  $y$  and the scale  $l$ .

From above mentioned fact and the streamwise constancy of the velocity defect, it is found that the velocity scale  $U$  and the length scale  $l$  are proportional to the  $-1/2$  power and  $1/2$  power of the streamwise distance  $x$ . Introducing a constant eddy viscosity, it is found that  $U$  and the Reynolds stress are proportional to a function  $f = \exp(-1/2 \cdot \alpha \xi^2)$  and  $-f'$  respectively. Where  $\xi = y/l$  and "" indicates the differentiation with respect to  $\xi$ .  $\alpha$  is a constant.

The turbulent intensity is thought to be proportional to the Reynolds stress. The shape of  $f'$  is shown in Fig.10.  $f'$  decreases near  $\xi = 0$ . This is not the case of the turbulent intensity, which has a nearly constant maximum value near  $\xi = 0$ .

### 6.2. Model of Turbulence Variation during One Wave Period

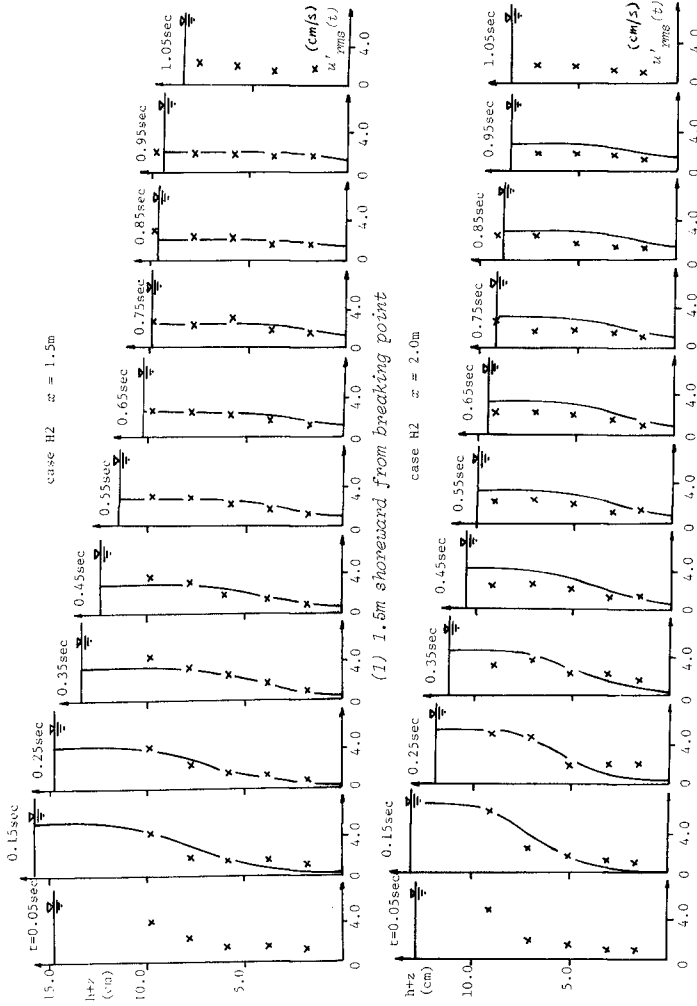


Fig. 8. (1), (2) Variation of Vertical Profile of Turbulent Intensity  $u'_{rms}(t)$  during One Wave Period

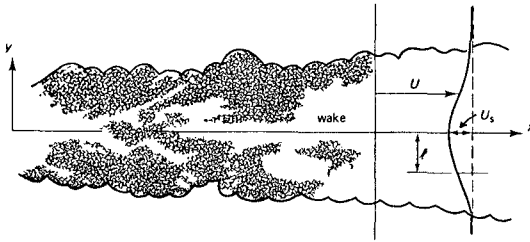


Fig.9 Turbulent Wake(Tennekes and Lumley, 1972)

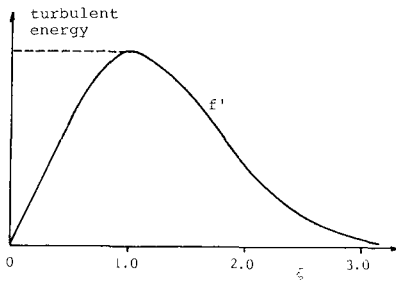


Fig.10 Lateral Profiles of Turbulence and Reynolds Stress(Tennekes and Lumley, 1972)

Before going to modeling, it should be noticed that the phenomenon to be modeled is the variation in time and not the variation in space. The turbulent wake theory itself explains the variation in the stream-wise direction. But this model does not treat the variation in the on-offshore direction.

The crest phase is taken as the time origin. The phase to be modeled is limited to the range from the crest to the following trough ( $t = t_p$ ).

The instantaneous water level at each phase is taken as corresponding to the center line  $y = 0$  of the turbulent wake(see Fig.9). The vertical distribution of the turbulence at each phase is assumed to be expressed by

$$\{u'_{rms}(z,t)\}^2 = \{u'_{rms}(t)_m\}^2 \gamma\{(\eta-z)/L\}, \tag{1}$$

in which  $\eta$  is the water level above the still water level, and  $L$  is the vertical length scale explained later. The function  $\gamma$  is assumed to be proportional to a function which takes the value expressed by the solid curve for  $\xi > 1.0$  and the peak value of the solid curve in Fig.10 for  $0 \leq \xi \leq 1.0$ .  $u'_{rms}(t)_m$  is a representative turbulent intensity at each phase(explained later).

The functional form of  $\gamma$  is determined by making its maximum value equal to 1.0 as follows :

$$\gamma(z) = \left( \begin{array}{l} \frac{\eta-z}{l} \exp\left(-\frac{1}{2}\left(\frac{\eta-z}{l}\right)^2 + \frac{1}{2}\right) ; \frac{\eta-z}{l} > 1.0 , \\ 1.0 ; 0 \leq \frac{\eta-z}{l} \leq 1.0 \end{array} \right) \quad (2)$$

The crest height  $\eta_0$  above the still water level is taken as the vertical length scale  $l_0$  at  $t = 0$ (crest phase). According to the turbulent wake theory,  $l$  is assumed to increase in proportion to the 1/2 power of the phase :

$$l = l_0 \{(t + T)/T\}^{1/2} , \quad (3)$$

where  $T$  is the wave period.

As seen from Eq. (3),  $l = l_0 = \eta_0$  at  $t = 0$ . So  $(\eta-z)/l = 1.0$  at  $t = 0$  and  $z = 0$ . Therefore at the crest phase,  $\gamma = 1.0$  from the water surface to the still water level. The measured value above the still water level at the crest phase should be taken as  $u'_{rms}(0)_m$ . Unfortunately there is no data above the still water level. The value of  $u'_{rms}(0)_m$  was estimated from the data at the highest point and the profile given by Eq.(2). According to the turbulent wake theory,  $u'_{rms}(t)_m$  is assumed to decrease in proportion to the -1/2 power of the phase :

$$\left\{ u'_{rms}(t)_m \right\}^2 = \left\{ u'_{rms}(0)_m \right\}^2 \left( \frac{1-K^2}{K^2} \frac{t + t_t}{t_t} \right)^{-1} , \quad (4)$$

where  $K = u'_{rms}(t_t)_m / u'_{rms}(0)_m$ .

The maximum measured value at  $t = t_t$  was taken as  $u'_{rms}(t_t)_m$ .

### 6.3. Comparison with Experimental Results

The phase 0.95sec after the zero-up crossing phase of the water surface was taken as  $t_t$ . The calculated vertical profile of the turbulent intensity is shown with solid lines in Fig. . The model developed here is rather simple. But the vertical profile and the time variation of the turbulence are explained well, at least in the lower part under the still water level.

But it should be recalled that the breaker type of the case H2 is a typical spilling type. Furthermore, the comparisons with the experimental results are limited to the data at the positions 1.5m and 2.0m shoreward from the breaking point. The width of the surf zone is about 500m. In these positions, the waves after breaking propagate just like stable bores. Therefore, it can be said that the model developed here is applicable to the turbulent field in the bore region located at 30 to 40% of the surf zone width shoreward from the breaking point.

## 7. CROSS PRODUCT OF ON-OFFSHORE AND VERTICAL DEVIATIONS

### 7.1. Result

Fig.11 shows the variation during one wave period of the ensemble averaged Reynolds stress  $\overline{\langle -u'w'(t) \rangle}$  at the location 1.5m shoreward from the breaking point in the case L, in which the two-components laser-doppler velocimeter was used. As explained in 3.3., the ensemble averaged Reynolds stress  $\overline{\langle -u'w'(t) \rangle}$  is defined as the ensemble average of the Reynolds stress  $-u'w'(t)$  at every 0.01sec of all waves during 48sec. But exactly speaking, the value shown in Fig.11 is not the value of this ensemble averaged Reynolds stress.

As explained in 3.3., the time interval of one wave period was defined as the interval from the phase 0.5sec after the preceeding wave crest to the phase of 0.5sec after the present wave crest. This time interval of one wave period was divided into 12 sections of 0.1sec. The value in Fig.11 is an averaged value of the ensemble averaged Reynolds stress in each section.

### 7.2. Discussions

One simple definition of Reynolds stress is the ensemble average of the product of the deviations  $u'$  and  $w'$  from the smoothed velocities over many waves. On the other hand, as well known, Reynolds stress is defined originally as a time mean of the product. So the Reynolds stress defined as the ensemble average over many waves is completely different from the original Reynolds stress.

In this study, the Reynolds stress was defined as the time mean. The interval of the time mean is 0.1sec(see 3.3.). The choice of the time length is arbitrary. There is no definite reason to choose 0.1sec. The time interval of no dropout is not always longer than 0.1sec. In a time interval shorter than 0.1sec, the interval of the time mean was reduced. Also in the beginning and end of one interval of no dropout, the interval of the time mean was reduced.

The number attached to each plotted point indicates the number of the averaged data. Near the water surface, it decreases rapidly. If no dropout occurs, it amounts to about 400.

The value itself is small compared with the value of the turbulent intensities  $u'_{rms}$ ,  $w'_{rms}$  and  $u'_{rms}(t)$  shown in Figs 6 to 8. In many points, it is smaller than  $1.0\text{cm}^2/\text{sec}^2$ .  $1.0\text{cm}^2/\text{sec}^2$  is the order of the possible error of the turbulent intensity(see 4.2.). At the position 0.5m shoreward from the breaking point, the calculated value of the ensemble averaged Reynolds stress in each section is less than  $0.5\text{cm}^2/\text{sec}^2$ . So, it may be said that the value of the Reynolds stress larger than  $0.5\text{cm}^2/\text{sec}^2$  is meaningful.

As explained in 6.1., the Reynolds stress in the turbulent wake is proportional to  $-f'$ . Therefore, the cross product itself is proportional



to  $f'$ . As shown in Fig.4 of Battjes and Sakai(1981), the cross product under a steady breaker generated behind a wing inserted in an open channel flow has a similar vertical profile as  $f'$  in Fig.10.

The direction of the positive on-offshore velocity in this study is opposite to that of the turbulent wake in Fig.9. So, if the Reynolds stress obeys the turbulent wake theory, it must be proportional to  $f'$ . In Fig.11, there is no such trend. It becomes negative in some parts of the vertical profile. It is also found that at the phase after the crest it has a positive hump in the lower part of the vertical profile.

As mentioned above, the calculated value of the Reynolds stress has many ambiguities. Therefore no definite conclusion is derived from Fig.11. Only thing to be said is that the Reynolds stress field in surf zone may not be explained by the turbulent wake theory which could explain roughly the turbulent intensity generated by wave breaking.

## 8. CONCLUSIONS

Horizontal and vertical velocities were measured with a hot-film anemometer and a two-components laser-doppler velocimeter in surf zones on uniform slopes of about 1/30 in two wave tanks.

The rectified on-offshore velocity measured with the hot-film anemometer was smoothed with a moving average method of 0.1sec. A root-mean-square of the deviation from the smoothed velocity was calculated for the onshore and offshore velocity phases of individual waves. The following conclusions were obtained : 1) The calculated turbulent intensity varies more and is larger in the case of the transient breaker type between spilling and plunging than in the case of spilling breaker, 2) the turbulent intensity does not damp so much as the waves propagate in the surf zone in the case of transient breaker, while it damps in the case of spilling breaker, and 3) the turbulent intensity is larger in the upper part of the water column than near the bottom.

A root-mean-square of the deviation from the smoothed on-offshore velocity was calculated for every 0.1sec section composing one wave period over about 20 waves in the case of spilling breaker. It was found that the vertical distribution of the calculated turbulent intensity and its variation during one wave period resemble those of the turbulence under a steady breaker generated behind a wing inserted in an open channel flow which was explained by the turbulent wake theory(Battjes and Sakai, 1981). A model was proposed, based on the turbulent wake theory, to explain the variation of the vertical distribution of turbulence during one wave period. It was found that this simple model can explain it roughly.

A time-mean over 0.1sec of the cross product of the on-offshore and vertical deviations from the smoothed values of the velocities measured with the laser-doppler velocimeter was calculated. It was defined as the Reynolds stress. An ensemble average of the Reynolds stress was

taken over about 40 waves. The variation during one wave period of the vertical distribution of the ensemble averaged Reynolds stress was discussed. It was suggested that the turbulent wake theory may not explain the variation of the Reynolds stress in surf zone.

#### 9. ACKNOWLEDGEMENT

This study was partly supported by the Grant-in-Aid for Scientific Research of the Ministry of Education, Science and Culture, Japan, for which the authors express their appreciation.

#### 10. REFERENCES

- Battjes, J.A. and T. Sakai (1981) : Velocity field in a steady breaker, Jour. of Fluid Mechanics, Vol.111, pp.421-437.
- Flick, R.E., R.T. Guza and D.L. Inman (1981) : Elevation and velocity measurements of laboratory shoaling waves, Jour. of Geophysical Research, Vol.86, No.C5, pp.4149-4160.
- Isobe, M., N. Fukuda and K. Horikawa (1979) : Experiment on velocity field in two-dimensional surf zone, Proc. of 26th Japanese Conf. on Coastal Engineering, p.42(in Japanese).
- Peregrine, D.H. and I.A. Svendsen (1978) : Spilling breakers, bores and hydraulic jumps, Proc. of 16th Conf. on Coastal Engineering, pp.540-550.
- Stive, M.J.F. (1980) : Velocity and pressure field of spilling breakers, Proc. of 17th Conf. on Coastal Engineering, pp.547-566.
- Tennekes, H. and J.L. Lumley (1972) : A First Course in Turbulence, The MIT Press, pp.104-145.